

1 ***Neisseria gonorrhoeae* scavenges host sialic acid for Siglec-mediated, complement-
2 independent suppression of neutrophil activation**

3

4 Amaris J Cardenas^a, Keena S. Thomas^a, Mary W. Broden^a, Noel J. Ferraro^b, Constance M.

5 John^c, Marcos M. Pires^b, Gary A. Jarvis^c, and Alison K. Criss^{a#}

6

7 ^aDepartment of Microbiology, Immunology, and Cancer Biology, University of Virginia,
8 Charlottesville, VA, USA

9 ^bDepartment of Chemistry, University of Virginia, Charlottesville, VA, USA

10 ^cVA Medical Center and University of California, San Francisco, San Francisco, CA, USA

11

12 Running title: Sialylated gonococci suppress neutrophils via Siglecs

13 #Corresponding author. Address: Box 800734, Charlottesville, VA, 22908-0734, USA. +1 434
14 243 3561; akc2r@virginia.edu

15 Keywords: *Neisseria gonorrhoeae*, gonorrhea, lipooligosaccharide, sialylation, neutrophils,
16 infection, reactive oxygen species, degranulation

17 Word Counts: Abstract – 218; Text – 4993

18 ABSTRACT

19 Gonorrhea, caused by the bacterium *Neisseria gonorrhoeae* (Gc), is characterized by neutrophil
20 influx to infection sites. Gc has developed mechanisms to resist killing by neutrophils that
21 include modifications to its surface lipooligosaccharide (LOS). One such LOS modification is
22 sialylation: Gc sialylates its terminal LOS sugars with cytidine-5'-monophosphate-N-
23 acetylneuraminic acid (CMP-NANA) scavenged from the host using LOS sialyltransferase (Lst),
24 since Gc cannot make its own sialic acid. Sialylation enables sensitive strains of Gc to resist
25 complement-mediated killing in a serum-dependent manner. However, little is known about the
26 contribution of sialylation to complement-independent, direct Gc-neutrophil interactions. In the
27 absence of complement, we found sialylated Gc expressing opacity-associated (Opa) proteins
28 decreased the oxidative burst and granule exocytosis from primary human neutrophils. In
29 addition, sialylated Opa+ Gc survived better than vehicle treated or Δ lst Gc when challenged
30 with neutrophils. However, Gc sialylation did not significantly affect Opa-dependent association
31 with or internalization of Gc by neutrophils. Previous studies have implicated sialic acid-binding
32 immunoglobulin-type lectins (Siglecs) in modulating neutrophil interactions with sialylated Gc.
33 Blocking neutrophil Siglecs with antibodies that bind to their extracellular domains eliminated the
34 ability of sialylated Opa+ Gc to suppress oxidative burst and resist neutrophil killing. These
35 findings highlight a new role for sialylation in Gc evasion of human innate immunity, with
36 implications for the development of vaccines and therapeutics for gonorrhea.

37 IMPORTANCE

38 *Neisseria gonorrhoeae*, the bacterium that causes gonorrhea, is an urgent global health concern
39 due to increasing infection rates, widespread antibiotic resistance, and its ability to thwart
40 protective immune responses. The mechanisms by which Gc subvert protective immune
41 responses remain poorly characterized. One way *N. gonorrhoeae* evades human immunity is by
42 adding sialic acid that is scavenged from the host onto its lipooligosaccharide, using the

43 sialyltransferase Lst. Here, we found that sialylation enhances *N. gonorrhoeae* survival from
44 neutrophil assault and inhibits neutrophil activation, independently of the complement system.
45 Our results implicate bacterial binding of sialic acid-binding lectins (Siglecs) on the neutrophil
46 surface, which dampen neutrophil antimicrobial responses. This work identifies a new role for
47 sialylation in protecting *N. gonorrhoeae* from cellular innate immunity, which can be targeted to
48 enhance the human immune response in gonorrhea.

49 INTRODUCTION

50 *Neisseria gonorrhoeae* (Gc) causes the bacterial sexually transmitted infection gonorrhea.
51 Gc is designated as an urgent threat level pathogen by the Centers for Disease Control and
52 Prevention, with approximately 82.4 million cases each year globally (1). Factors contributing to
53 the prevalence of gonorrhea include increasing resistance to antibiotics, resistance to soluble
54 and cellular innate immune components, and the lack of protective immunity elicited by prior
55 infection (2, 3). Finding new approaches to treat or prevent Gc infection is of utmost importance.

56 The most abundant surface component on Gc is lipooligosaccharide (LOS). The length and
57 composition of LOS is regulated by *lgt* (LOS glycosyltransferase) genes. Phase variation of *lgt*
58 genes results in varying oligosaccharide (OS) compositions within a Gc population, including
59 during infection (4-7). Gc isolated from uncomplicated urethral infection predominantly produce
60 LOS that can be sialylated. Sialylation is the incorporation of sialic acid onto the alpha and/or
61 beta chain terminal galactose of LOS, catalyzed by Gc LOS sialyltransferase (Lst) (8-10). Gc
62 cannot synthesize sialic acid and instead scavenges CMP-NANA from the host (11). Lst is
63 constitutively expressed (12, 13), is required for optimal genital tract infection (14-16), and uses
64 diverse forms of CMP-sialic acid (17).

65 LOS sialylation is a form of molecular mimicry by which Gc is thought to evade immune
66 recognition (18, 19). Sialylation was originally characterized as conferring "unstable" serum
67 resistance on Gc recovered from urethral secretions, but not after lab passage (11, 20, 21).

68 Sialylation has since been shown to inhibit all three complement activation pathways by
69 decreasing C1 engagement and C4b deposition, and increasing recruitment of factor H on Gc
70 (17, 22, 23). Sialylated glycans enable the immune system to discriminate self from non-self,
71 achieved in part through sialic acid-binding immunoglobulin-type lectins (Siglecs) (24-27).
72 Siglecs are produced by most immune cells, including neutrophils, which are the predominant
73 immune cells recruited in Gc infections and constitute the purulence in gonorrhreal secretions
74 (28). Human neutrophils express Siglec-5, -9, and -14. Siglec-5 and -9 contain cytoplasmic
75 immunoreceptor tyrosine-based inhibitory motifs (ITIMs) that recruit SH2 domain-containing
76 phosphatases to inhibit cellular activation (29-34). In contrast, Siglec-14 associates with the
77 adapter protein DAP12, which contains an immunoreceptor tyrosine-based activating motif
78 (ITAM) that once phosphorylated, recruits Syk kinase to activate downstream signaling (35, 36).
79 The genes that encode Siglec-5 and Siglec-14 are adjacent and considered paired receptors,
80 since the proteins share almost complete sequence identity in their binding domains and similar
81 glycan binding preferences (35, 37). 10-70% of individuals in certain racial/ethnic groups harbor
82 a *SIGLEC14/5* fusion gene where Siglec-14 is not expressed, but Siglec-5 is (38). Thus, on
83 balance, signaling through neutrophil Siglecs dampens inflammatory signaling. Sialylated Gc
84 has been reported to interact with recombinant extracellular domains of these Siglecs (39).

85 Gc expresses numerous gene products that defend against neutrophil antimicrobial activities
86 (28). Gc also varies its ability to interact non-opsonically with neutrophils through phase-variable
87 expression of opacity-associated (Opa) proteins (40). Most Opa proteins bind one or more
88 carcinoembryonic antigen-related cell adhesion molecules (CEACAMs). In particular, binding to
89 the granulocyte-restricted CEACAM3 elicits phagocytosis, reactive oxygen species production,
90 and granule release (41-47).

91 In this study, we unexpectedly found that sialylation promotes Gc survival from human
92 neutrophils in a complement-independent manner. Our results implicate Siglecs in dampening

93 the neutrophil activation that is elicited by CEACAM-binding Opa proteins, bringing new insight
94 into the ways that Gc modulates soluble and cellular human innate immunity to persist in its
95 obligate human host.

96 **RESULTS**

97 **Gc Lst incorporates sialic acid onto LOS, which is retained upon infection of neutrophils.**

98 To investigate the role of LOS sialylation on direct, nonopsonic Gc interactions with
99 neutrophils, we first assessed Lst- and CMP-NANA-dependent sialylation of Opa-expressing
100 (Opa+) Gc. The wild-type (WT) Lst parent for these studies was a derivative of strain FA1090 1-
101 81-S2 that constitutively expresses the OpaD protein in an otherwise Opa-negative background,
102 hereafter termed OpaD (48). OpaD binds CEACAMs 1 and 3 on human neutrophils, leading to
103 rapid phagocytic killing (48, 49). This strain produces the sialylatable lacto-N-neotetraose
104 (LNnT) alpha chain and lactose beta chain (50). OpaD was transformed with insertionally
105 inactivated *lst* to generate an isogenic mutant that cannot be sialylated (OpaDΔ/*lst*) (15).
106 Bacteria were incubated with CMP-NANA or vehicle control, then washed to remove residual
107 sialic acid and processed for downstream analysis.

108 Monoclonal antibody (mAb) 6B4 binds the LNnT epitope of the alpha chain of *Neisseria* LOS;
109 α2,3 sialylation of its terminal galactose prevents 6B4 binding (8, 51). By Western blot, 6B4
110 reacted with lysates of OpaD, and binding was lost when OpaD was incubated with CMP-NANA
111 (**Fig 1A**). 6B4 reacted with OpaDΔ/*lst* lysates with or without CMP-NANA (**Fig 1A**). To analyze
112 sialylation on individual bacteria, we used imaging flow cytometry with 6B4. The fluorescence
113 index of OpaD incubated with CMP-NANA was significantly lower than OpaD without CMP-
114 NANA and OpaDΔ/*lst* with or without CMP-NANA; these three were statistically indistinguishable
115 (**Fig 1B-C**).

116 Two other sialylation sites on LOS have been reported in Gc: the P^k-like alpha chain (18, 52)
117 and the lactose-bearing beta chain (50, 53), both through α2,6 linkage. To directly detect Lst-

118 dependent sialylation on Gc LOS, independent of 6B4 exclusion, we applied copper click
119 chemistry using azido-labeled sialic acid, followed by alkyne-FITC cycloaddition (54-57). OpaD
120 incorporated CMP-Azido (Az)-NANA in a Lst-dependent manner (**Fig 1D-E**), which was
121 displaced in competition with unmodified CMP-NANA at approximately equimolar concentration
122 (**Fig 1F**). Using Gc preincubated with CMP-Az-NANA, we monitored the retention of sialylation
123 on OpaD in the presence of neutrophils. Representative images collected at 30 min post-
124 infection showed alkyne-FITC labeled bacteria that were both intracellularly and extracellularly
125 attached to neutrophils (**Fig 1G**). Thus, imaging flow cytometry, in combination with
126 immunofluorescence and click chemistry, can be used to track and quantify Gc LOS sialylation
127 alone and in cells.

128 **Lst-dependent sialylation of Opa+ Gc dampens human neutrophil activation and protects**
129 **Gc from killing by neutrophils**

130 We explored the contribution of Gc Lst-dependent sialylation to neutrophil activation. First,
131 the release of reactive oxygen species (ROS) was measured. As previously reported,
132 nonsialylated OpaD elicited robust neutrophil ROS production (**Fig 2A-B**) (42, 45, 48).
133 Sialylation significantly reduced the magnitude of the OpaD-elicited oxidative burst; ROS
134 production was inversely correlated with the concentration of CMP-NANA for sialylation (**Fig 2A-**
135 **B**). Sialylation similarly reduced the oxidative burst in response to other Opa+ bacteria (**Fig 2C**,
136 **Fig S1A**). OpaD Δ /st elicited neutrophil ROS production regardless of CMP-NANA addition, and
137 was indistinguishable from nonsialylated OpaD (**Fig 2D**, **Fig S1B**).

138 ROS does not directly contribute to neutrophil antigenococcal activity (58-60), ROS
139 production requires intracellular signaling events and granule release (61). Neutrophil granules
140 contain antimicrobial components, some of which are bactericidal for Gc (62-64). Thus, we
141 analyzed the effect of sialylation on the ability of OpaD to stimulate exocytosis of primary and
142 secondary neutrophil granules as measured by CD63 and CD66b surface presentation,

143 respectively (42). Sialylation of Gc significantly reduced neutrophil exocytosis of primary (**Fig.**
144 **2E**) and secondary (**Fig 2F**) granules at 30 min post-infection. Together, these data indicate
145 sialylation reduces the ability of Gc to activate neutrophils.

146 We next tested the contribution of Lst-dependent sialylation to bacterial survival in the
147 presence of adherent, IL-8 primed primary human neutrophils without addition of human serum
148 (complement). Sialylated OpaD had a statistically significant increase in survival over
149 nonsialylated bacteria at 15 and 30 min postinfection (**Fig 3A**). OpaD Δ/st phenocopied
150 nonsialylated OpaD at these times, showing that both sialic acid and Lst were required for the
151 increased survival of OpaD exposed to neutrophils. By 60 and 120 min post-infection, survival of
152 sialylated OpaD was not statistically different from nonsialylated Gc (**Fig 3A**). Sialylation also
153 significantly increased the survival from neutrophils of CEACAM-binding Opa60+ Gc, through 2
154 h infection (**Fig 3B**). However, survival of Opaless Gc from neutrophils was unaffected by
155 sialylation, which fits with our previous reports that Opa-negative Gc persist in the presence of
156 neutrophils (48, 59, 65) (**Fig 3C**). These results highlight a role for Lst-dependent sialylation in
157 survival of Opa+ Gc from neutrophils.

158 **Sialylation of LOS does not directly affect OpaD-CEACAM3 interactions**

159 Given the importance of CEACAM3 to phagocytic killing of Opa+ Gc by neutrophils, we
160 tested the hypothesis that Gc sialylation disrupted OpaD-CEACAM3 engagement. First,
161 sialylated or nonsialylated OpaD was incubated with a Glutathione S-transferase (GST)-tagged
162 N-terminus of human CEACAM3 (N-CEACAM3), and CEACAM3 binding was measured by flow
163 cytometry using anti-GST fluorescence (66). Lst-dependent sialylation did not significantly affect
164 OpaD binding of N-CEACAM3 (**Fig 4A**). Sialylation also did not affect interaction of OpaD with
165 N-CEACAM1 (**Fig S2**). Opaless Gc, which does not bind CEACAMs, served as negative
166 control. Second, association of sialylated or nonsialylated OpaD with human CEACAM-3
167 transfected CHO cells was measured by imaging flow cytometry. Lst-dependent sialylation did

168 not significantly affect bacterial association with hCEACAM3-CHO cells (**Fig 4B**). These results
169 indicate that contrary to our hypothesis, sialylation does not affect Opa-CEACAM engagement.

170 In a previous report, sialylation decreased the adherence of Opa+ Gc to neutrophils in
171 suspension, but this effect was lost over time (67). We thus hypothesized that the mechanism
172 by which sialylated Gc resisted killing by neutrophils was due to decreased association with
173 and/or internalization by these immune cells. To test this hypothesis, we used imaging flow
174 cytometry (68), in which extracellular Gc were discriminated from intracellular bacteria by
175 accessibility of a mAb against FA1090 PorB1b. Binding of this antibody to Gc was unaffected by
176 sialylation (**Fig S3**). Sialylation did not significantly affect OpaD association with (**Fig 4C**) or
177 internalization by (**Fig 4D**) neutrophils through 30 min post-infection, when effects were
178 measured by ROS production and bacterial survival. We conclude that sialylation does not
179 directly affect Opa+ Gc interaction with neutrophil CEACAMs.

180 **Sialylated Gc bind immunoregulatory Siglecs to dampen neutrophil activation and
181 antigenococcal activity**

182 The inhibitory effect of Gc sialylation on neutrophil activation and not phagocytosis, along
183 with work from other groups (37, 39, 69, 70), led us to investigate the contribution of sialic acid
184 immunoglobulin-type lectins (Siglecs). Using imaging flow cytometry, we confirmed the
185 presence of Siglec-9 and Siglec-5/14 on the surface of primary human neutrophils (**Fig 5A**)
186 compared to unstained (**Fig S4A**). Staining ranged from small puncta to rings around the cell
187 periphery, though there was minimal overlap in Siglec-9 vs. Siglec-5/14 localization (**Fig 5B**).

188 We hypothesized that sialic acid-Siglec engagement interfered with Opa-CEACAM binding to
189 dampen the neutrophil response to Opa+ Gc. To test this, neutrophils were incubated with
190 blocking antibodies against the extracellular domains of Siglec-9 and -5/14 (71), then exposed
191 to sialylated or nonsialylated OpaD, and ROS production was measured. As seen in **Fig 2**,
192 sialylation significantly reduced the neutrophil oxidative burst in response to OpaD when isotype

193 control antibodies were added (purple bars, **Fig 5C**). Addition of anti-Siglec antibodies
194 significantly enhanced the burst elicited by sialylated OpaD (solid green vs. solid purple, **Figs**
195 **5C** and **S4B**), restoring it to levels that were no different from unsialylated OpaD. The
196 restoration of ROS in the presence of Siglec-blocking antibodies was specific to sialylated Gc,
197 as nonsialylated OpaD induced similar levels of ROS whether or not blocking antibodies were
198 present (green outline vs. purple outline, **Fig. 5D**). These data implicate Siglecs in the ability of
199 sialylated Opa+ Gc to reduce neutrophil activation.

200 The dampened ROS release in response to sialylated Opa+ Gc led us to examine if blocking
201 Siglecs restored the ability of neutrophils to control Opa+ bacteria. Neutrophils were incubated
202 with blocking antibodies against Siglec-9 and -5/14 or left untreated, then exposed to sialylated
203 or nonsialylated OpaD. Addition of anti-Siglec antibodies significantly reduced the survival of
204 sialylated OpaD after infection of neutrophils at 15 and 30 min, to a level equivalent to
205 nonsialylated OpaD (**Fig 5D**). Nonsialylated OpaD were recovered similarly from neutrophils
206 whether or not anti-Siglec antibodies were present, indicating that the effect of Siglecs on Gc-
207 neutrophil interaction is specific to sialylated Gc.

208 From these results, we conclude that Gc uses sialylation of its LOS in a Siglec-mediated,
209 complement-independent manner to impede neutrophil activation and antigenococcal
210 responses, thereby promoting bacterial survival during infection.

211 **DISCUSSION**

212 Gc sialylation of LOS by Lst is crucial for complement resistance and pathogenesis *in vivo*
213 (10). This study reveals an unexpected, complement-independent role of sialylation: its ability to
214 restrain neutrophil activation in response to Opa+ Gc, improving Gc survival upon neutrophil
215 challenge. Sialylation reduced granule mobilization and release of both oxidative and
216 nonoxidative species in response to Opa+ bacteria. Unexpectedly, sialylation of the LOS did not
217 markedly affect Opa-CEACAM engagement. Instead, by blocking the immunoregulatory Siglecs

218 on neutrophils, sialylated Opa+ Gc could no longer suppress neutrophil activation or killing
219 capacity. These data suggest the exploitation of neutrophil self-associated molecular pattern
220 recognition by Gc through LOS sialylation by Lst. Our findings add to the increasing
221 understanding of how pathogens co-opt host factors to impair immune cell activation (72).

222 This study focused on Gc interactions with neutrophils, the main cell type found in human
223 infectious secretions. We used human neutrophils that were adherent and treated with IL-8,
224 mimicking post-migration behavior in these terminally differentiated, short-lived primary cells
225 (59). Work by our group and others has investigated how Gc expression of phase-variable Opa
226 proteins affects its survival from neutrophils (40-42, 45, 48, 63, 73). Most Opa proteins bind
227 selected human CEACAMs. In particular, neutrophils and other granulocytes express
228 CEACAM3, which contains an ITAM that can recruit Src family and Syk tyrosine kinases to drive
229 signaling pathways leading to phagocytosis, granule release, and ROS production (40). Given
230 the negative charge conferred by sialic acids, we hypothesized that LOS sialylation would impair
231 the phagocytic activity of neutrophils towards Gc. However, we found no significant difference in
232 the ability of sialylated Opa+ Gc to bind the soluble N-domain of CEACAM, CEACAM-
233 expressing cells, or primary human neutrophils. While our study only focused on Opa+ Gc that
234 bind CEACAMs 1 and 3, future work can explore how sialylation affects other modes of
235 interaction between Gc and neutrophils, including antibody- and complement-mediated
236 association.

237 Siglecs help the innate immune system to distinguish between non-self and self-associated
238 molecular patterns (26). Many immune cell Siglecs contain cytoplasmic ITIM domains that
239 transduce inhibitory signals to dampen inflammation (24). Other sialylated bacteria, including *N.*
240 *meningitidis* and Group B *Streptococcus*, have been shown to manipulate cell activation via
241 Siglec engagement (27, 69), and Gc can bind human Siglec-Fc chimera proteins (39).
242 Consistent with published findings, we detected Siglec-9 and Siglec-5/14 on the human
243 neutrophil surface (29, 32, 37). Moreover, blocking Siglecs reversed the inhibitory activity of

244 sialylation on neutrophil responses to Gc, uncovering a new role for Siglecs in thwarting
245 neutrophil antigenococcal responses. Interestingly, human Siglec-Fc chimeras have also been
246 reported to bind PorB on the surface of unsialylated Gc, which was enhanced by production of a
247 shorter, nonsialylatable LOS (39). Whether nonsialylated Gc interact with Siglecs on neutrophils
248 and the consequences of such interaction remain to be explored. Unlike Siglec-5 and Siglec-9,
249 Siglec-14 does not have a cytoplasmic domain; instead, it associates with the ITAM-bearing
250 DAP12 (35, 37). Siglec-5 and Siglec-14 have almost identical ligand binding domains due to
251 ongoing gene conversion and are considered paired receptors, possibly to balance immune
252 responses to pathogens (24, 35, 38). In a study of genetic variations in Siglecs among a human
253 cohort with a high burden of gonorrhea, uninfected individuals were more likely to produce
254 Siglec-14, though not reaching statistical significance (39). Future work can examine if
255 neutrophils from individuals with or without Siglec-14 respond differently to sialylated Gc.

256 The localization of Lst has recently been updated from an outer membrane protein to the
257 inner face of the cytoplasmic membrane, where the OS is assembled (74, 75). Unlike the
258 closely related microbe *N. meningitidis*, Gc cannot endogenously synthesize CMP-NANA and
259 must scavenge it from the extracellular environment for sialylation. Lst has both α 2,3 (alpha
260 chain LNnT) and α 2,6 sialyltransferase activity (alpha chain P^k-like OS and beta chain lactose)
261 and has been shown to use different CMP-sialic acids as substrates (8, 17, 52, 53). This
262 promiscuity suggests that sialic acid availability rather than enzymatic activity drives the
263 dynamics of LOS sialylation. We exploited this feature of Lst to add azido-labeled CMP-NANA in
264 the form of N-acetylneuraminic acid (Neu5Ac) to directly track sialylation on the Gc surface.
265 Other Lst substrates include CMP-Neu5Gc, which is missing in humans due to the evolutionary
266 loss of the responsible hydrolase (76), and CMP-legionaminic acid and CMP-
267 ketodeoxynonulosonic acid, which do not confer complement-resistance and could serve as
268 antigenococcal therapeutics (17).

269 One key question prompted by this work is how neutrophils affect the dynamics of Gc

270 sialylation. Neutrophils have been proposed as a source of CMP-NANA, since lysates from
271 polymorphonuclear phagocytes, including neutrophils, confer “unstable” serum resistance on Gc
272 (77). How Gc obtains CMP-NANA, which is cytoplasmic, is currently unknown, since
273 intracellular Gc reside in phagolysosomes (65). Phagosomes may contain sialic acid
274 transporters; in addition, neutrophils may release CMP-NANA by lysis or elaboration of
275 neutrophil extracellular traps. It is also tantalizing to speculate that neutrophil sialyltransferases,
276 found in the secretory pathway, could intersect with Gc- and sialic acid-containing
277 compartments to sialylate the bacteria (78). Conversely, neutrophils have surface-exposed
278 sialidases, which desialylate their own glycans during diapedesis (79, 80) and other cells'
279 glycans for adhesion (81). While we did not detect any desialylation of Gc over the first 30 min
280 of neutrophil exposure, the sialylation state of Gc over time with neutrophils remains unknown.
281 Modification of neutrophil-like cells to synthesize azido-labeled CMP-NANA (82) would allow
282 sialylation of Gc to be tracked over time and in different

283 Sialylated Gc have reduced infectivity in experimental challenge of the human male urethra
284 (14) and in the genital tract of female mice (15, 16). However, Gc isolated from male urethral
285 gonorrheal exudates are sialylated (8, 11, 21). Additionally, Gc isolated from cervicovaginal
286 human secretions are less likely to be sialylated, due to sialidase activity conferred by members
287 of the female genital microbiome (83). Given these dynamics, we anticipate that balancing
288 sialylation state allows Gc to resist cellular and humoral immunity – including by engaging
289 Siglecs to thwart neutrophil attack – while maintaining infectivity of target mucosal surfaces.
290 These findings can be exploited for novel therapies for gonorrhea, since Lst expression is not
291 phase variable. For instance, CMP-NANA analogs that do not confer serum resistance aid
292 complement killing of multidrug-resistant Gc (17, 84). Similarly, sialic acid analogs that do not
293 engage Siglecs could be developed to render Gc more sensitive to neutrophils. These
294 approaches, in conjunction with antibiotics and vaccines, could enhance neutrophil and soluble
295 host defenses to combat drug-resistant gonorrhea.

296 **MATERIALS AND METHODS**

297 **Bacterial strains and growth conditions**

298 Gc in this study are in the FA1090 background, constitutively expressing the pilin variant 1-81-
299 S2 and with in-frame deletions of all *opa* genes (Opaless) (48). Opaless Gc with non-phase
300 variable, constitutively expressed *opaD* has been described previously (OpaD) (48); Opa60 and
301 Opal were constructed similarly (49, 66).

302 Gc were grown overnight on gonococcal medium base (Difco) with Kellogg's supplements
303 (85) (GCB) at 37°C with 5% CO₂. Growth of Gc in rich liquid medium containing Kellogg's
304 supplements and NaHCO₃ to enrich for pilated, live, mid-logarithmic phase bacteria has been
305 previously described (86). For sialylation, 50µg/mL of cytidine-5'-monophosphate-N-
306 acetylneuraminic acid (CMP-NANA) (Nacalai) reconstituted in PBS was added for the final 2.5 h
307 growth (87). Gc were washed with PBS + 5mM MgSO₄ prior to infection. CMP-Az-NANA (R&D
308 Systems) was added in lieu of or in competition with unmodified CMP-NANA (54).

309 Isogenic OpaDΔ/st was generated by spot transforming OpaD with genomic DNA from MS11
310 GP300 *lst*::Kan (from A. Jerse, USUHS) (15). Transformants were selected on GCB with
311 50µg/mL kanamycin and confirmed by PCR, and inability to sialylate OpaDΔ/st was verified by
312 6B4 exclusion (see below). OpaD expression was confirmed by Western blotting bacterial
313 lysates with 4B12 mAb against Opa (88, 89).

314 **Gc sialylation and detecting sialylated Gc**

315 Western blot: SDS-PAGE and immunoblotting for 6B4 reactivity was conducted as previously
316 described (17). In brief, lysates from Gc with or without CMP-NANA pre-incubation, were
317 resolved using a 4-20% gradient SDS-polyacrylamide gel (Bio-Rad) and transferred in CAPS
318 methanol buffer to polyvinylidene difluoride (PVDF). Membranes were blocked in PBS + 0.5%
319 Tween-20 + 5% dry skim milk and probed with 6B4 tissue culture supernatant (from S. Ram,
320 UMass) followed by anti-mouse IgM-horseradish peroxidase (HRP) antibody (Jackson

321 ImmunoResearch). Blots were developed with SuperSignal chemiluminescent substrate
322 (ThermoFisher). For imaging flow cytometry, Gc (10^8 CFU/mL), incubated with or without
323 50 μ g/mL CMP-NANA, were labeled with 5 μ M Tag-IT Violet (TIV) (BioLegend) then incubated
324 with 6B4, followed by AlexaFluor647-coupled goat anti-mouse IgM (Jackson ImmunoResearch)
325 before fixation and processing. Samples were examined using ImageStream X Mark II imaging
326 flow cytometer and analyzed using INSPIRE and IDEAS v. 6.2 software packages (Amnis
327 Luminex Corporation). Focused, singlet TIV+ Gc were gated as in (66). AF647+ gate was set in
328 reference to TIV+ Gc without 6B4. Data are reported as fluorescence index (geometric mean
329 fluorescence intensity x percent AF647+).

330 Click chemistry: Gc (10^8 CFU/mL) with or without CMP-Az-NANA were stained with TIV
331 before fixation to analyze Gc alone, or used to infect primary human neutrophils at a multiplicity
332 of infection (MOI) of 1 (see below). After fixation with 2% paraformaldehyde (PFA), neutrophils
333 were incubated with H.5 mouse anti-PorB (from M. Hobbs, UNC) to detect extracellular Gc, then
334 permeabilized with 0.2% saponin. Copper-catalyzed click chemistry was carried out for 1 hr at
335 room temperature with continuous shaking, using reaction reagents: 2.5mM THPTA (tris-
336 hydroxypropyltriazolylmethylamine) ligand (Lumiprobe), 0.06mM FAM alkyne 5-isomer (5-
337 Carboxyfluorescein) (Lumiprobe), 2.4 mM L-ascorbic acid (VWR), and 2mM copper (II) sulfate
338 pentahydrate all dissolved in UltraPure distilled water (Invitrogen) (90). Samples were
339 thoroughly washed before analysis by imaging flow cytometry.

340 **Neutrophil isolation**

341 Human subjects research was conducted in accordance with a protocol approved by the
342 University of Virginia Institutional Review Board for Health Sciences Research (#13909).
343 Informed, formal written consent was obtained from each participant. Neutrophils were isolated
344 from venous blood collected from healthy human subjects via dextran sedimentation followed by
345 a Ficoll gradient as described (86). Neutrophils were resuspended in Dulbecco's phosphate

346 buffered saline (DPBS; without calcium and magnesium; Thermo Scientific) with 0.1% dextrose
347 and used within 1 h after isolation. Samples were > 95% neutrophils and > 99% viable.

348 **Neutrophil ROS production**

349 Neutrophils were resuspended in Morse's Defined Medium (MDM) (91) containing 20 μ M
350 luminol. Gc was added at an MOI of 100 and the generation of reactive oxygen species was
351 measured every 3 min for 1 h via chemiluminescence (86). Negative controls included Opaless-
352 infected and uninfected neutrophils (48). Line graphs are one representative of three or more
353 biological replicates. Bar graphs present all biological replicates' area under the curve (AUC)
354 values.

355 **Neutrophil granule exocytosis**

356 Surface expression of neutrophil granule proteins was measured as in (42), using phycoerythrin
357 (PE)-CD63 for primary granules and allophycocyanin (APC)-CD66b for secondary granules (or
358 isotype controls PE-IgG1 and APC-IgM) (BioLegend). Data were acquired using a Cytek
359 Northern Lights spectral flow cytometer and analyzed using FCS Express (De Novo Software).
360 The median fluorescence of each sample was normalized to unstimulated neutrophils as
361 negative control.

362 **Gc survival in the presence of neutrophils**

363 Infection of adherent, IL-8 treated human neutrophils in RPMI 1640 medium with 10% heat-
364 inactivated fetal bovine serum (HI-FBS) was conducted as in (86), except Gc was pre-incubated
365 with or without CMP-NANA. After centrifugation to synchronize infection and incubation at 37°C,
366 5% CO₂, neutrophils were lysed with 1% saponin, serially diluted, and plated for overnight
367 growth on GCB. Results are reported as percentage of CFUs enumerated from lysates at the
368 indicated timepoint, divided by CFUs enumerated at 0 min.

369 **Imaging flow cytometric analysis of Gc association with and internalization by**
370 **neutrophils**

371 Infection of primary human neutrophils with TIV+ Gc and evaluation by imaging flow cytometry
372 was performed as described (42, 68, 92). Because sialylation reduced bacterial binding of the
373 goat anti-Gc antibody (Biosource) to almost undetectable levels (data not shown), extracellular
374 Gc were recognized instead with H.5 anti-PorB, followed by AF647-coupled goat anti-mouse
375 antibody.

376 **NCEACAM-1 and NCEACAM-3 binding of Opa expressing Gc**

377 GST-tagged N-terminal domains of human CEACAMs 1 and 3 were purified and utilized as in
378 (66). In brief, nonsialylated or sialylated Gc were incubated with GST-N-CEACAM1 or -N-
379 CEACAM3 for 30 min at 37°C with end-over-end rotation. Gc were washed and incubated with
380 mouse anti-GST antibody p1A12 (BioLegend) followed by an AF488-conjugated goat anti-
381 mouse antibody (Jackson ImmunoResearch). The percentage of AF488+ (N-CEACAM-bound)
382 Gc was measured using imaging flow cytometry.

383 **Gc association with CHO-hCEACAM-1 and -3 cells**

384 hCEACAM1-, hCEACAM3-, and Control-CHOs were generated using heparan-sulfate
385 proteoglycan deficient Chinese hamster ovary (CHO) cell strain PgsD-677 (ATCC). Cells were
386 grown in Ham's F-12K medium (ATCC) with HI-FBS and 1x Antibiotic-Antimycotic (Gibco) at
387 37°C, 5% CO₂. Plasmids were prepared from VectorBuilder *Escherichia coli* stocks using
388 Plasmid Miniprep (Qiagen) and ampicillin selection: human CEACAM1 (VB900000-5687rxc),
389 human CEACAM3 (VB900000-7471zkb), or an empty control (VB010000-9288rhy) vector under
390 a CAG promoter. CHOs were transfected using Lipofectamine 3000 transfection reagent
391 (Invitrogen) according to manufacturer instructions. After 48 h, transfectants were selected using
392 10µg/mL puromycin (Gibco). A non-transfected control was used to confirm selection.
393 Transfectants were maintained under puromycin selection throughout culturing and passaged at

394 70-90% confluence; medium was replaced with antibiotic-free medium 2 h prior to infection.
395 Surface expression of CEACAM on pooled CEACAM1- and 3-CHO transfectants, and absence
396 on Control-CHOs, were confirmed by immunofluorescence microscopy using anti-Pan-CEACAM
397 antibody (Abcam, clone D14HD11).

398 Cells were seeded in a 6-well plate and grown for 48 hr to confluence ($\sim 10^6$ cells/well). TIV+
399 Gc were added at an MOI of 1 to cells on ice, centrifuged to synchronize infection, washed, and
400 incubated for 30 min. Cells were lifted with Versene solution (Gibco) at 37°C, 5% CO₂ for 10
401 min. Cells were then fixed with 2% PFA, collected with a rubber cell scraper, and filtered through
402 50 μ m nylon mesh. Cells were blocked in PBS + 10% normal goat serum and incubated with
403 anti-Pan-CEACAM antibody followed by goat anti-mouse AF555-conjugated antibody
404 (Invitrogen). Cells were analyzed using imaging flow cytometry and IDEAS software. Focused
405 cells were gated by gradient root mean square for image sharpness ≥ 50 . Single cells were
406 gated by high aspect ratio and area ≥ 200 and ≤ 1000 . Single stained controls were used to set
407 gates for AF555+ and TIV+ populations.

408 **Siglec staining and blockade**

409 Adherent, IL-8 primed neutrophils were fixed and lifted with a cell scraper then cells were
410 washed in PBS and blocked in 10% normal goat serum. Next, neutrophils were incubated with
411 anti-Siglec-9-APC (Clone 191240) and/or anti-Siglec-5/14-AF488 (Clone 194128) (R&D
412 Systems) for 30 min. Samples were analyzed using imaging flow cytometry as above. To block
413 Siglecs, isolated neutrophils were incubated with the unconjugated forms of anti-Siglec-9 and/or
414 anti-Siglec-5/14 for 30 min at 37°C + 5% CO₂ before infection.

415 **Statistics**

416 Results are depicted as the means \pm standard errors for ≥ 3 independent experiments. Statistics
417 were calculated using GraphPad Prism; a *p* value of ≤ 0.05 was considered significant. Analysis

418 of variance (ANOVA) or mixed model analysis was used for multiple comparisons for parametric
419 data.

420 **Acknowledgements**

421 This work was supported by NIH R01AI097312, NIH U19AI144180, and NIH U01AI162457
422 (AKC). AJC was supported in part by NIH F31AI157528 and NIH 3R01AI097312-07S1. AJC
423 and MWB were supported in part by NIH T32AI007046. MMP and NJF were supported by NIH
424 R35GM124893. GAJ and CMJ were supported by Merit Review Award BX000727 and
425 Research Career Scientist Award from the Research Service of the US Department of Veterans
426 Affairs. The funders had no role in study design, data collection and interpretation, or the
427 decision to submit the work for publication. We thank Louise Ball and Samuel Clark for
428 preliminary experiments that informed this project, and Asya Smirnov and Linda Columbus for
429 experimental advice. We thank Mike Solga of the UVA Flow Cytometry Core Facility
430 (RRid:SCR_017829) and Hazel Ozuna (University of Louisville) for advice, Ann Jerse and
431 Marcia Hobbs for strains and antibodies, and Sanjay Ram for reagents and discussions. We
432 thank the human subjects who make this research possible.

433

434 **Author contributions**

435 Conceptualization: AJC, AKC. Formal analysis: AJC, KST, NJF. Funding acquisition: AKC, AJC,
436 GAJ, MMP. Project Administration: AKC. Investigation: AJC, KST, MWB, CMJ, NJF.
437 Methodology: AJC, MWB, NJF, CMJ, MMP. Supervision: GAJ, MMP, AKC. Visualization: AJC.
438 Writing – original draft: AJC, AKC. Writing – review & editing: AJC, KST, MWB, NJF, CMJ, MMP,
439 GAJ, AKC.

440 **References**

- 441 1. World Health Organization. 18 July 2023. Gonorrhoea (*Neisseria gonorrhoeae*
442 infection). [https://www.who.int/news-room/fact-sheets/detail/gonorrhoea-\(neisseria-gonorrhoeae-infection\)](https://www.who.int/news-room/fact-sheets/detail/gonorrhoea-(neisseria-gonorrhoeae-infection)). Accessed Jan 10 2024.

- 444 2. Workowski KA, Bachmann LH, Chan PA, Johnston CM, Muzny CA, Park I, Reno H,
445 Zenilman JM, Bolan GA. 2021. Sexually transmitted infections treatment guidelines,
446 2021. MMWR Recomm Rep.
- 447 3. Rice PA, Shafer WM, Ram S, Jerse AE. 2017. *Neisseria gonorrhoeae*: Drug Resistance,
448 Mouse Models, and Vaccine Development. Annu Rev Microbiol 71:665-686.
- 449 4. Yamasaki R, Bacon BE, Nasholds W, Schneider H, Griffiss JM. 1991. Structural
450 determination of oligosaccharides derived from lipooligosaccharide of *Neisseria*
451 *gonorrhoeae* F62 by chemical, enzymatic, and two-dimensional NMR methods.
452 Biochemistry 30:10566-75.
- 453 5. John CM, Griffiss JM, Apicella MA, Mandrell RE, Gibson BW. 1991. The Structural Basis
454 for Pyocin Resistance in *Neisseria gonorrhoeae* Lipooligosaccharides. J Biol Chem
455 266:19303-19311.
- 456 6. Gotschlich EC. 1994. Genetic locus for the biosynthesis of the variable portion of
457 *Neisseria gonorrhoeae* lipooligosaccharide. J Exp Med 180:2181-90.
- 458 7. Tong Y, Arking D, Ye S, Reinhold B, Reinhold V, Stein DC. 2002. *Neisseria gonorrhoeae*
459 strain PID2 simultaneously expresses six chemically related lipooligosaccharide
460 structures. Glycobiology 12:523-33.
- 461 8. Apicella MA, Mandrell RE, Shero M, Wilson ME, Griffiss JM, Brooks GF, Lammel C,
462 Breen JF, Rice PA. 1990. Modification by sialic acid of *Neisseria gonorrhoeae*
463 lipooligosaccharide epitope expression in human urethral exudates: an immunoelectron
464 microscopic analysis. J Infect Dis 162:506-12.
- 465 9. Mandrell RE, Smith H, Jarvis GA, Griffiss JM, Cole JA. 1993. Detection and some
466 properties of the sialyltransferase implicated in the sialylation of lipopolysaccharide of
467 *Neisseria gonorrhoeae*. Microb Pathog 14:307-313.
- 468 10. Ram S, Shaughnessy J, de Oliveira RB, Lewis LA, Gulati S, Rice PA. 2017. Gonococcal
469 lipooligosaccharide sialylation: virulence factor and target for novel immunotherapeutics.
470 Pathog Dis 75.
- 471 11. Nairn CA, Cole JA, Patel PV, Parsons NJ, Fox JE, Smith H. 1988. Cytidine 5'-
472 monophospho-N-acetylneuraminic acid or a related compound is the low Mr factor from
473 human red blood cells which induces gonococcal resistance to killing by human serum. J
474 Gen Microbiol 134:3295-306.
- 475 12. Gilbert M, Watson DC, Cunningham AM, Jennings MP, Young NM, Wakarchuk WW.
476 1996. Cloning of the lipooligosaccharide alpha-2,3-sialyltransferase from the bacterial
477 pathogens *Neisseria meningitidis* and *Neisseria gonorrhoeae*. J Biol Chem 271:28271-6.
- 478 13. Packiam M, Shell DM, Liu SV, Liu YB, McGee DJ, Srivastava R, Seal S, Rest RF. 2006.
479 Differential expression and transcriptional analysis of the alpha-2,3-sialyltransferase
480 gene in pathogenic *Neisseria* spp. Infect Immun 74:2637-50.

- 481 14. Schneider H, Schmidt KA, Skillman DR, Van De Verg L, Warren RL, Wylie HJ, Sadoff
482 JC, Deal CD, Cross AS. 1996. Sialylation Lessens the Infectivity of *Neisseria*
483 *gonorrhoeae* MS11mkC. *J Infect Dis* 173:1422-1427.
- 484 15. Wu H, Jerse AE. 2006. Alpha-2,3-sialyltransferase enhances *Neisseria gonorrhoeae*
485 survival during experimental murine genital tract infection. *Infect Immun* 74:4094-103.
- 486 16. Lewis LA, Gulati S, Burrowes E, Zheng B, Ram S, Rice PA. 2015. alpha-2,3-
487 sialyltransferase expression level impacts the kinetics of lipooligosaccharide sialylation,
488 complement resistance, and the ability of *Neisseria gonorrhoeae* to colonize the murine
489 genital tract. *MBio* 6:e02465-14.
- 490 17. Gulati S, Schoenhofen IC, Whitfield DM, Cox AD, Li J, St Michael F, Vinogradov EV,
491 Stupak J, Zheng B, Ohnishi M, Unemo M, Lewis LA, Taylor RE, Landig CS, Diaz S,
492 Reed GW, Varki A, Rice PA, Ram S. 2015. Utilizing CMP-Sialic Acid Analogs to Unravel
493 *Neisseria gonorrhoeae* Lipooligosaccharide-Mediated Complement Resistance and
494 Design Novel Therapeutics. *PLoS Pathog* 11:e1005290.
- 495 18. Mandrell RE, Griffiss JM, Macher BA. 1988. Lipooligosaccharides (LOS) of *Neisseria*
496 *gonorrhoeae* and *Neisseria meningitidis* have components that are immunochemically
497 similar to precursors of human blood group antigens. Carbohydrate sequence specificity
498 of the mouse monoclonal antibodies that recognize crossreacting antigens on LOS and
499 human erythrocytes. *J Exp Med* 168:107-26.
- 500 19. Mandrell RE. 1992. Further Antigenic Similarities of *Neisseria gonorrhoeae*
501 Lipooligosaccharides and Human Glycosphingolipids. *Infect Immun* 60:3017-3020.
- 502 20. Ward ME, Watt PJ, Glynn AA. 1970. Gonococci in urethral exudates possess a virulence
503 factor lost on subculture. *Nature* 227:382-384.
- 504 21. Martin PM, Patel PV, Parsons NJ, Smith H. 1982. Induction in gonococci of phenotypic
505 resistance to killing by human serum by human genital secretions. *Br J Vener Dis*
506 58:363-5.
- 507 22. Ram S, Sharma AK, Simpson SD, Gulati S, McQuillen DP, Pangburn MK, Rice PA. 1998.
508 A novel sialic acid binding site on factor H mediates serum resistance of sialylated
509 *Neisseria gonorrhoeae*. *J Exp Med* 187:743-52.
- 510 23. Gulati S, Sastry K, Jensenius JC, Rice PA, Ram S. 2002. Regulation of the mannan-
511 binding lectin pathway of complement on *Neisseria gonorrhoeae* by C1-inhibitor and
512 alpha 2-macroglobulin. *J Immunol* 168:4078-86.
- 513 24. Pillai S, Netravali IA, Cariappa A, Mattoo H. 2012. Siglecs and immune regulation. *Annu*
514 *Rev Immunol* 30:357-92.
- 515 25. Macauley MS, Crocker PR, Paulson JC. 2014. Siglec-mediated regulation of immune
516 cell function in disease. *Nat Rev Immunol* 14:653-66.
- 517 26. Laubli H, Varki A. 2020. Sialic acid-binding immunoglobulin-like lectins (Siglecs) detect
518 self-associated molecular patterns to regulate immune responses. *Cell Mol Life Sci*
519 77:593-605.

- 520 27. Carlin AF, Chang YC, Areschoug T, Lindahl G, Hurtado-Ziola N, King CC, Varki A, Nizet
521 V. 2009. Group B *Streptococcus* suppression of phagocyte functions by protein-
522 mediated engagement of human Siglec-5. *J Exp Med* 206:1691-9.
- 523 28. Palmer A, Criss AK. 2018. Gonococcal Defenses against Antimicrobial Activities of
524 Neutrophils. *Trends Microbiol* 26:1022-1034.
- 525 29. Cornish AL, Freeman S, Forbes G, Ni J, Zhang M, Cepeda M, Gentz R, Augustus M,
526 Carter KC, Crocker PR. 1998. Characterization of Siglec-5, a Novel Glycoprotein
527 Expressed on Myeloid Cells Related to CD33. *Blood* 92:2123-2132.
- 528 30. Avril T, Freeman SD, Attrill H, Clarke RG, Crocker PR. 2005. Siglec-5 (CD170) can
529 mediate inhibitory signaling in the absence of immunoreceptor tyrosine-based inhibitory
530 motif phosphorylation. *J Biol Chem* 280:19843-51.
- 531 31. Erickson-Miller CL, Freeman SD, Hopson CB, D'Alessio KJ, Fischer EI, Kikly KK,
532 Abrahamson JA, Holmes SD, King AG. 2003. Characterization of Siglec-5 (CD170)
533 expression and functional activity of anti-Siglec-5 antibodies on human phagocytes. *Exp
534 Hematol* 31:382-8.
- 535 32. Avril T, Floyd H, Lopez F, Vivier E, Crocker PR. 2004. The membrane-proximal
536 immunoreceptor tyrosine-based inhibitory motif is critical for the inhibitory signaling
537 mediated by Siglecs-7 and -9, CD33-related Siglecs expressed on human monocytes
538 and NK cells. *J Immunol* 173:6841-9.
- 539 33. Lizcano A, Secundino I, Dohrmann S, Corriden R, Rohena C, Diaz S, Ghosh P, Deng L,
540 Nizet V, Varki A. 2017. Erythrocyte sialoglycoproteins engage Siglec-9 on neutrophils to
541 suppress activation. *Blood* 129:3100-3110.
- 542 34. Delaveris CS, Wilk AJ, Riley NM, Stark JC, Yang SS, Rogers AJ, Ranganath T, Nadeau
543 KC, Stanford C-B, Blish CA, Bertozzi CR. 2021. Synthetic Siglec-9 Agonists Inhibit
544 Neutrophil Activation Associated with COVID-19. *ACS Cent Sci* 7:650-657.
- 545 35. Angata T, Hayakawa T, Yamanaka M, Varki A, Nakamura M. 2006. Discovery of Siglec-
546 14, a novel sialic acid receptor undergoing concerted evolution with Siglec-5 in primates.
547 *FASEB J* 20:1964-73.
- 548 36. Lanier LL, Bakker ABH. 2000. The ITAM-bearing transmembrane adaptor DAP12 in
549 lymphoid and myeloid cell function. *Immunol Today* 21:611-614.
- 550 37. Ali SR, Fong JJ, Carlin AF, Busch TD, Linden R, Angata T, Areschoug T, Parast M, Varki
551 N, Murray J, Nizet V, Varki A. 2014. Siglec-5 and Siglec-14 are polymorphic paired
552 receptors that modulate neutrophil and amnion signaling responses to group B
553 *Streptococcus*. *J Exp Med* 211:1231-42.
- 554 38. Yamanaka M, Kato Y, Angata T, Narimatsu H. 2009. Deletion polymorphism of
555 SIGLEC14 and its functional implications. *Glycobiology* 19:841-6.
- 556 39. Landig CS, Hazel A, Kellman BP, Fong JJ, Schwarz F, Agarwal S, Varki N, Massari P,
557 Lewis NE, Ram S, Varki A. 2019. Evolution of the exclusively human pathogen *Neisseria*

- 558 *gonorrhoeae*: Human-specific engagement of immunoregulatory Siglecs. *Evol Appl*
559 12:337-349.
- 560 40. Sadarangani M, Pollard AJ, Gray-Owen SD. 2011. Opa proteins and CEACAMs:
561 pathways of immune engagement for pathogenic *Neisseria*. *FEMS Microbiol Rev*
562 35:498-514.
- 563 41. Gray-Owen SD, Dehio C, Haude A, Grunert F, Meyer T, F. 1997. CD66 carcinoembryonic
564 antigens mediate interactions between Opa-expressing *Neisseria gonorrhoeae* and
565 human polymorphonuclear phagocytes. *EMBO J* 16:3435-3445.
- 566 42. Alcott AM, Werner LM, Baiocco CM, Dufrisne MB, Columbus L, Criss AK. 2022. Variable
567 Expression of Opa Proteins by *Neisseria gonorrhoeae* Influences Bacterial Association
568 and Phagocytic Killing by Human Neutrophils. *J Bacteriol* 204: e0003522.
- 569 43. Bos MP, Kao D, Hogan DM, Grant CC, Belland RJ. 2002. Carcinoembryonic antigen
570 family receptor recognition by gonococcal Opa proteins requires distinct combinations of
571 hypervariable Opa protein domains. *Infect Immun* 70:1715-23.
- 572 44. Popp A, Dehio C, Grunert F, Meyer TF, Gray-Owen SD. 1999. Molecular analysis of
573 neisserial Opa protein interactions with the CEA family of receptors: identification of
574 determinants contributing to the differential specificities of binding. *Cell Microbiol* 1:169-
575 81.
- 576 45. Smirnov A, Daily KP, Criss AK. 2014. Assembly of NADPH oxidase in human neutrophils
577 is modulated by the opacity-associated protein expression state of *Neisseria*
578 *gonorrhoeae*. *Infect Immun* 82:1036-44.
- 579 46. Sarantis H, Gray-Owen SD. 2007. The specific innate immune receptor CEACAM3
580 triggers neutrophil bactericidal activities via a Syk kinase-dependent pathway. *Cell*
581 *Microbiol* 9:2167-80.
- 582 47. Buntru A, Roth A, Nyffenegger-Jann NJ, Hauck CR. 2012. HemITAM signaling by
583 CEACAM3, a human granulocyte receptor recognizing bacterial pathogens. *Arch*
584 *Biochem Biophys* 524:77-83.
- 585 48. Ball LM, Criss AK. 2013. Constitutively Opa-expressing and Opa-deficient *Neisseria*
586 *gonorrhoeae* strains differentially stimulate and survive exposure to human neutrophils. *J*
587 *Bacteriol* 195:2982-90.
- 588 49. Martin JN, Ball LM, Solomon TL, Dewald AH, Criss AK, Columbus L. 2016. Neisserial
589 Opa Protein-CEACAM Interactions: Competition for Receptors as a Means of Bacterial
590 Invasion and Pathogenesis. *Biochemistry* 55:4286-94.
- 591 50. John CM, Phillips NJ, Cardenas AJ, Criss AK, Jarvis GA. 2023. Comparison of
592 lipooligosaccharides from human challenge strains of *Neisseria gonorrhoeae*. *Front*
593 *Microbiol* 14:1215946.
- 594 51. Mandrell RE, Schneider H, Apicella MA, Zollinger W, Rice PA, Griffiss JM. 1986.
595 Antigenic and physical diversity of *Neisseria gonorrhoeae* lipooligosaccharides. *Infect*
596 *Immun* 54:63-9.

- 597 52. Wakarchuk WW, Gilbert M, Martin A, Wu Y, Brisson JR, Thibault P, Richards JC. 1998.
598 Structure of an alpha-2,6-sialylated lipooligosaccharide from *Neisseria meningitidis*
599 immunotype L1. *Eur J Biochem* 254:626-33.
- 600 53. Ram S, Gulati S, Lewis LA, Chakraborti S, Zheng B, DeOliveira RB, Reed GW, Cox AD,
601 Li J, St Michael F, Stupak J, Su XH, Saha S, Landig CS, Varki A, Rice PA. 2018. A Novel
602 Sialylation Site on *Neisseria gonorrhoeae* Lipooligosaccharide Links Heptose II Lactose
603 Expression with Pathogenicity. *Infect Immun* 86.
- 604 54. Wu ZL, Huang X, Burton AJ, Swift KA. 2015. Glycoprotein labeling with click chemistry
605 (GLCC) and carbohydrate detection. *Carbohydr Res* 412:1-6.
- 606 55. Han Z, Thuy-Boun PS, Pfeiffer W, Vartabedian VF, Torkamani A, Teijaro JR, Wolan DW.
607 2021. Identification of an N-acetylneurameric acid-presenting bacteria isolated from a
608 human microbiome. *Sci Rep* 11:4763.
- 609 56. Goon S, Schilling B, V. TM, Gibson BW, Bertozzi CR. 2003. Metabolic incorporation of
610 unnatural sialic acids into *Haemophilus ducreyi* lipooligosaccharides. *Proc Natl Acad Sci*
611 USA 100:3089-94.
- 612 57. Feigman MS, Kim S, Pidgeon SE, Yu Y, Ongwae GM, Patel DS, Regen S, Im W, Pires
613 MM. 2018. Synthetic Immunotherapeutics against Gram-negative Pathogens. *Cell Chem*
614 *Biol* 25:1185-1194 e5.
- 615 58. Casey SG, Shafer WM, Spitznagel JK. 1986. *Neisseria gonorrhoeae* Survive
616 Intraleukocytic Oxygen-Independent Antimicrobial Capacities of Anaerobic and Aerobic
617 Granulocytes in the Presence of Pyocin Lethal for Extracellular Gonococci. *Infect Immun*
618 52:384-9.
- 619 59. Criss AK, Katz BZ, Seifert HS. 2009. Resistance of *Neisseria gonorrhoeae* to non-
620 oxidative killing by adherent human polymorphonuclear leucocytes. *Cell Microbiol*
621 11:1074-87.
- 622 60. Seib KL, Simons MP, Wu HJ, McEwan AG, Nauseef WM, Apicella MA, Jennings MP.
623 2005. Investigation of oxidative stress defenses of *Neisseria gonorrhoeae* by using a
624 human polymorphonuclear leukocyte survival assay. *Infect Immun* 73:5269-72.
- 625 61. Nguyen GT, Green ER, Mecsas J. 2017. Neutrophils to the ROScue: Mechanisms of
626 NADPH Oxidase Activation and Bacterial Resistance. *Front Cell Infect Microbiol* 7:373.
- 627 62. Rest RF. 1979. Killing of *Neisseria gonorrhoeae* by Human Polymorphonuclear
628 Neutrophil Granule Extracts. *Infect Immun* 25:574-579.
- 629 63. Johnson MB, Ball LM, Daily KP, Martin JN, Columbus L, Criss AK. 2015. Opa+ *Neisseria*
630 *gonorrhoeae* exhibits reduced survival in human neutrophils via Src family kinase-
631 mediated bacterial trafficking into mature phagolysosomes. *Cell Microbiol* 17:648-65.
- 632 64. Shafer WM, Martin LE, Spitznagel JK. 1986. Late intraphagosomal hydrogen ion
633 concentration favors the in vitro antimicrobial capacity of a 37-kilodalton cationic granule
634 protein of human neutrophil granulocytes. *Infect Immun* 53:651-5.

- 635 65. Johnson MB, Criss AK. 2013. *Neisseria gonorrhoeae* phagosomes delay fusion with
636 primary granules to enhance bacterial survival inside human neutrophils. *Cell Microbiol*
637 15:1323-40.
- 638 66. Werner LM, Palmer A, Smirnov A, Belcher Dufrisne M, Columbus L, Criss AK. 2020.
639 Imaging Flow Cytometry Analysis of CEACAM Binding to Opa-Expressing *Neisseria*
640 *gonorrhoeae*. *Cytometry A* 97:1081-9.
- 641 67. Rest RF, Frangipane JV. 1992. Growth of *Neisseria gonorrhoeae* in CMP-N-
642 acetylneuraminic acid inhibits nonopsonic (opacity-associated outer membrane protein-
643 mediated) interactions with human neutrophils. *Infect Immun* 60:989-97.
- 644 68. Smirnov A, Solga MD, Lannigan J, Criss AK. 2020. Using Imaging Flow Cytometry to
645 Quantify Neutrophil Phagocytosis. *Methods Mol Biol* 2087:127-140.
- 646 69. Jones C, Virji M, Crocker PR. 2003. Recognition of sialylated meningococcal
647 lipopolysaccharide by siglecs expressed on myeloid cells leads to enhanced bacterial
648 uptake. *Molecular Microbiology* 49:1213-1225.
- 649 70. Graustein AD, Horne DJ, Fong JJ, Schwarz F, Mefford HC, Peterson GJ, Wells RD,
650 Musvosvi M, Shey M, Hanekom WA, Hatherill M, Scriba TJ, Thuong NTT, Mai NTH,
651 Caws M, Bang ND, Dunstan SJ, Thwaites GE, Varki A, Angata T, Hawn TR. 2017. The
652 SIGLEC14 null allele is associated with *Mycobacterium tuberculosis*- and BCG-induced
653 clinical and immunologic outcomes. *Tuberculosis (Edinb)* 104:38-45.
- 654 71. Kelm S, Pelz A, Schauer R, Filbin MT, Tang S, de Bellard ME, Schnaar RL, Mahoney JA,
655 Hartnell A, Bradfield P, Crocker PR. 1994. Sialoadhesin, myelin-associated glycoprotein
656 and CD22 define a new family of sialic acid-dependent adhesion molecules of the
657 immunoglobulin superfamily. *Curr Biol* 4:965-972.
- 658 72. Werner LM, Criss AK. 2023. Diverse Functions of C4b-Binding Protein in Health and
659 Disease. *J Immunol* 211:1443-9.
- 660 73. Islam EA, Anipindi VC, Francis I, Shaik-Dasthagirisaheb Y, Xu S, Leung N, Sintsova A,
661 Amin M, Kaushic C, Wetzler LM, Gray-Owen SD. 2018. Specific Binding to Differentially
662 Expressed Human Carcinoembryonic Antigen-Related Cell Adhesion Molecules
663 Determines the Outcome of *Neisseria gonorrhoeae* Infections along the Female
664 Reproductive Tract. *Infect Immun* 86:e00092-18.
- 665 74. Shell DM, Chiles L, Judd RC, Seal S, Rest RF. 2002. The *Neisseria* lipooligosaccharide-
666 specific alpha-2,3-sialyltransferase is a surface-exposed outer membrane protein. *Infect*
667 *Immun* 70:3744-51.
- 668 75. Jen FE, Ketterer MR, Semchenko EA, Day CJ, Seib KL, Apicella MA, Jennings MP.
669 2021. The Lst Sialyltransferase of *Neisseria gonorrhoeae* Can Transfer Keto-
670 Deoxyoctanoate as the Terminal Sugar of Lipooligosaccharide: a Glyco-Achilles Heel
671 That Provides a New Strategy for Vaccines to Prevent Gonorrhea. *mBio* 12:e00092-18.
- 672 76. Chou HH, Hayakawa T, Diaz S, Krings M, Indriati E, Leakey M, Paabo S, Satta Y,
673 Takahata N, Varki A. 2002. Inactivation of CMP-N-acetylneuraminic acid hydroxylase

- 674 occurred prior to brain expansion during human evolution. Proc Natl Acad Sci USA
675 99:11736-41.
- 676 77. Patel PV, Parsons NJ, Andrade JRC, Nairn CA, Tan EL, Goldner M, Cole JA, Smith H.
677 1988. White blood cells including polymorphonuclear phagocytes contain a factor which
678 induces gonococcal resistance to complement-mediated serum killing. FEMS Microbiol
679 Lett 50:173-6.
- 680 78. Eckhardt M, Gotza B, Gerardy-Schahn R. 1999. Membrane Topology of the Mammalian
681 CMP-Sialic Acid Transporter. J Biol Chem 274:8779-87.
- 682 79. Cross AS, Wright DG. 1991. Mobilization of sialidase from intracellular stores to the
683 surface of human neutrophils and its role in stimulated adhesion responses of these
684 cells. J Clin Invest 88:2067-76.
- 685 80. Rifat S, Kang TJ, Mann D, Zhang L, Puche AC, Stamatos NM, Goldblum SE, Brossmer
686 R, Cross AS. 2008. Expression of sialyltransferase activity on intact human neutrophils.
687 J Leukoc Biol 84:1075-81.
- 688 81. Sakarya S, Rifat S, Zhou J, Bannerman DD, Stamatos NM, Cross AS, Goldblum SE.
689 2004. Mobilization of neutrophil sialidase activity desialylates the pulmonary vascular
690 endothelial surface and increases resting neutrophil adhesion to and migration across
691 the endothelium. Glycobiology 14:481-94.
- 692 82. Hong V, Steinmetz NF, Manchester M, Finn MG. 2010. Labeling live cells by copper-
693 catalyzed alkyne--azide click chemistry. Bioconjug Chem 21:1912-6.
- 694 83. Ketterer MR, Rice PA, Gulati S, Kiel S, Byerly L, Fortenberry JD, Soper DE, Apicella MA.
695 2016. Desialylation of *Neisseria gonorrhoeae* Lipooligosaccharide by Cervicovaginal
696 Microbiome Sialidases: The Potential for Enhancing Infectivity in Men. J Infect Dis
697 214:1621-8.
- 698 84. Gulati S, Schoenhofen IC, Lindhout-Djukic T, Lewis LA, Moustafa IY, Saha S, Zheng B,
699 Nowak N, Rice PA, Varki A, Ram S. 2020. Efficacy of Antigonococcal CMP-
700 Nonulosonate Therapeutics Require Cathelicidins. J Infect Dis 222:1641-50.
- 701 85. Kellogg DS, Peacock WL, Deacon WE, Brown L, Pirkle DI. 1963. *Neisseria*
702 *gonorrhoeae*. I. Virulence genetically linked to clonal variation. J Bacteriol
703 85:1274-9.
- 704 86. Ragland SA, Criss AK. 2019. Protocols to Interrogate the Interactions Between *Neisseria*
705 *gonorrhoeae* and Primary Human Neutrophils. Methods Mol Biol 1997:319-45.
- 706 87. Gulati S, Rice PA, Ram S. 2019. Complement-Dependent Serum Bactericidal Assays for
707 *Neisseria gonorrhoeae*. Methods Mol Biol 1997:267-80.
- 708 88. Achtman M, Neibert M, Crowe BA, Strittmatter W, Kusecek B, Weyse E, Walsh MJ,
709 Slawig B, Morelli G, Moll A. 1988. Purification and characterization of eight class 5 outer
710 membrane protein variants from a clone of *Neisseria meningitidis* serogroup A. J Exp
711 Med 168:507-25.

- 712 89. Geslewitz WE, Cardenas AJ, Zhou X, Zhang Y, Criss AK, Seifert HS. 2023. Development
713 and implementation of a Type I-C CRISPR-based programmable repression system for
714 *Neisseria gonorrhoeae*. MBio doi:10.1128/mbio.03025-23:e0302523.
- 715 90. Ferraro NJ, Kim S, Im W, Pires MM. 2021. Systematic Assessment of Accessibility to the
716 Surface of *Staphylococcus aureus*. ACS Chem Biol 16:2527-36.
- 717 91. Morse S, Bartenstein L. 1980. Purine metabolism in *Neisseria gonorrhoeae*: the
718 requirement for hypoxanthine. Can J Microbiol 26:13-20.
- 719 92. Werner LM, Alcott A, Mohlin F, Ray JC, Belcher Dufrisne M, Smirnov A, Columbus L,
720 Blom AM, Criss AK. 2023. *Neisseria gonorrhoeae* co-opts C4b-binding protein to
721 enhance complement-independent survival from neutrophils. PLoS Pathog
722 19:e1011055.

723

724 **Figure Legends**

725 **Figure 1. Analysis and quantification of Lst-dependent sialylation of gonococcal**
726 **lipooligosaccharide. (A)** OpaD and OpaD Δ /lst were grown with 50 μ g/mL CMP-Neu5Ac (NANA)
727 (+) or vehicle (Veh) (-). Bacterial lysates were Western blotted with mAb 6B4, or anti-Zwf as
728 loading control, followed by HRP-conjugated secondary antibodies. Blot is representative of n=3
729 biological replicates. **(B-C)** OpaD and OpaD Δ /lst were incubated with CMP-NANA or vehicle as
730 in **A**, then stained with Tag-IT Violet (TIV). Bacteria were incubated with 6B4 followed by
731 AlexaFluor647-coupled secondary antibody, fixed, and analyzed by imaging flow cytometry. **(B)**
732 Average fluorescence index (FI: mean fluorescence intensity (MFI) x percent positive) from n=3
733 biological replicates with 20,000 events collected per condition; each symbol indicates one
734 matched biological replicate. Statistical analysis by one-way ANOVA with Tukey's multiple
735 comparisons test. **=p \leq 0.01. **(C)** Representative images for the indicated condition; AF647-6B4
736 signal is false-colored orange, and yellow numbers indicate the object's fluorescence intensity
737 value. **(D-G)** Gc were incubated with either CMP-NANA and/or CMP-Az-NANA at 100ng/mL.
738 Bacteria were stained with TIV, fixed, then subjected to copper catalyzed click chemistry azide-
739 alkyne cycloaddition using fluorescein isothiocyanate (FITC)-alkyne. **(D)** Representative images
740 of CMP-NANA and CMP-Az-NANA sialylated OpaD, each of which was subjected to alkyne-

741 FITC cycloaddition. Yellow numbers are as in **C**. **(E)** OpaD or OpaD Δ /st were incubated with
742 indicated concentrations of CMP-Az-NANA or CMP-NANA. The MFI of each condition was
743 quantified from flow cytometry, n=1. **(F)** WT OpaD was incubated with 0.1 μ g/mL of CMP-Az-
744 NANA along with the indicated concentration of unmodified CMP-NANA. Results are graphed
745 as the MFI of each condition and fit with a non-linear regression line. **(G)** OpaD sialylated with
746 CMP-Az-NANA was stained with TIV and used to infect IL-8 treated, adherent primary human
747 neutrophils for 30 min. After fixation, extracellular Gc were labeled with anti-PorB and AF647-
748 coupled secondary antibody (false-colored cyan) before permeabilization with 0.1% saponin
749 followed by copper click chemistry. Representative images of infected neutrophils with
750 intracellular (TIV+AF647-) and extracellular (TIV+AF647+) Gc with azide-sialylated LOS that is
751 clicked with the alkyne-FITC probe (FITC+).

752

753 **Figure 2. Sialylation dampens neutrophil activation in response to Opa+ bacteria. (A-B)**
754 OpaD incubated with the indicated concentrations of CMP-NANA or vehicle (0 μ g/mL) were
755 exposed to primary human neutrophils in the presence of luminol at an MOI of 100. Neutrophil
756 oxidative burst was measured as relative light units (RLUs) of luminol-dependent
757 chemiluminescence every 3 min over 1 h. **(A)** displays one representative graph of n=4; **(B)** is
758 the average \pm SEM area under the curve (AUC) for each condition across replicates (symbols
759 indicate matched biological replicates). **(C)** Opa60 Gc (blue) or Opal Gc (orange) were
760 incubated with 50 μ g/mL CMP-NANA (+) or vehicle (-) before neutrophil exposure; AUCs of n=4
761 biological replicates. Non-stimulatory Opaless Gc (dark grey) exposed neutrophils or neutrophils
762 (PMNs) in luminol alone (light grey) serve as negative controls. **(D)** WT (purple) or Δ /st (red)
763 OpaD were treated with or without CMP-NANA then added to neutrophils as above; AUCs of
764 n=3 biological replicates. Statistical analyses by one-way ANOVA with Tukey's multiple
765 comparisons test. * $=p\leq 0.05$; ** $=p\leq 0.01$. **(E-F)** OpaD treated with CMP-NANA or vehicle as

766 above were added to adherent, IL-8 primed neutrophils for 15 or 30 min at an MOI of 1.
767 Neutrophils were stained for viability (Zombie Near Infrared) and with a PE-coupled antibody
768 against primary granule protein CD63 (**E**) and an APC-coupled antibody against secondary
769 granule protein CD66b (**F**) on the cell surface. After fixation, cells were analyzed via spectral
770 flow cytometry. Data are presented as median fluorescence (Med Fl) of PE+ (**E**) and APC+ (**F**)
771 live cells, gated using unstained and isotype controls. Results are from n=4 biological replicates
772 (symbol matched). Statistical analyses were performed by two-way ANOVA with Šídák's
773 multiple comparisons test. *= $p \leq 0.05$.

774 **Figure 3. Sialylated, Opa+ bacteria have a survival advantage at early times of neutrophil
775 challenge.** Adherent, IL-8 primed neutrophils were infected with sialylated (filled) or
776 nonsialylated (empty) (**A**) OpaD (purple) or OpaDΔ/st (red), at a MOI of 1. Gc viability was
777 determined by the enumeration of CFUs from lysed neutrophils at the indicated times post-
778 infection, expressed as a percentage of CFU at 0 min. (**B-C**) Sialylated and nonsialylated
779 Opa60 Gc (blue) (**B**) and Opaless Gc (grey) (**C**) were exposed to neutrophils and bacterial
780 viability measured as in **A**. Results are presented as the average \pm SEM for n \geq 3 (**A**) n=4 (**B**) or
781 n=3 (**C**) biological replicates, matched by symbol within each data set. Statistical comparisons
782 were by mixed effect analysis (**A**) or two-way ANOVA (**B-C**) with Holm-Šídák's multiple
783 comparisons test with the following pairwise significances: *= $p \leq 0.05$; **= $p \leq 0.01$; ****= $p \leq 0.0001$.

784 **Figure 4. Sialylation does not affect binding of OpaD bacteria to CEACAM-3.** (**A**) OpaD
785 grown with CMP-NANA or vehicle were incubated with GST-tagged recombinant N-terminal
786 domain of CEACAM-3 (NCEACAM-3). Binding of NCEACAM-3 to Gc was detected using a
787 mouse anti-GST antibody, followed by a goat anti-mouse IgG AF488-conjugated antibody. Gc
788 were fixed, stained with DAPI, and analyzed by imaging flow cytometry, to calculate the percent
789 of singlet Gc that are AF488+. Opaless Gc that does not bind CEACAM is shown as a negative
790 control (grey). (**B**) CHO cells transfected with human CEACAM3 (hCCM3) or empty control

791 vector (Ctrl Vec) were infected with TIV-labeled OpaD, treated with CMP-NANA or vehicle. After
792 30 min, cells were collected, stained with a pan-CEACAM antibody followed by AF555-
793 conjugated secondary antibody, and fixed. The percent of singlet CHO cells that are TIV+
794 (infected) was calculated using imaging flow cytometry. Results are from n=3 biological
795 replicates (symbol matched). Statistical comparisons were by two-way ANOVA with Tukey's
796 multiple comparisons test; not significant. **(C-D)** OpaD with or without sialylated LOS were
797 labeled with TIV and used to infect adherent, IL-8 primed neutrophils. At the indicated time
798 points, infected cells were fixed and extracellular Gc were detected with an anti-PorB antibody,
799 followed by an AF488-coupled secondary antibody, without permeabilization. Cells were then
800 analyzed using imaging flow cytometry to report the percent of neutrophils with associated
801 (%TIV+) Gc **(C)** or internalized (%TIV+AF488-) Gc **(D)**. Results are from n=4 biological
802 replicates (symbol matched). Statistical comparisons were by two-way ANOVA with Tukey's
803 multiple comparisons test; not significant.

804

805 **Figure 5. Blockade of neutrophil Siglec-9 and Siglec-5/14 reverses the ability of sialylated**
806 **gonococci to suppress neutrophil activation and antibacterial activity. (A-B)** Uninfected
807 and adherent, IL-8 primed human neutrophils were incubated with antibodies that recognize
808 human Siglec-9-APC and/or Siglec-5/Siglec-14-AF488 antibodies, without cell permeabilization
809 before fixation and processing via imaging flow cytometry. **(A)** Dot plot of focused singlet
810 neutrophils with anti-Siglec-9(APC) and anti-Siglec-5/14(AF488). X axis indicates AF488
811 fluorescence intensity and y axis indicates APC fluorescence intensity. Double positive (green)
812 gate based on single stains; number within gate is the percent of the stained condition. **(B)**
813 Representative images of neutrophils stained with anti-Siglec-9-APC (cyan) and anti-Siglec-
814 5/14-AF488 (yellow); colored fluorescence in merged. Results are representative of n=3
815 biological replicates by spectral flow cytometry and confocal microscopy (not shown) and

816 demonstrate n=1 replicate with imaging flow cytometry. **(C-D)** Primary human neutrophils were
817 incubated with anti-human Siglec-9 and Siglec-5/-14 antibodies (green) or media alone (purple)
818 for 30 min. **(C)** Neutrophils were then exposed to sialylated (filled) or nonsialylated (empty)
819 OpaD at an MOI of 100 in the presence of luminol. ROS production was measured over 1 h by
820 luminol-dependent chemiluminescence as RLU. Graphed data of AUCs for each condition
821 across n=6 biological replicates (symbol matched). Statistical comparisons by one-way ANOVA
822 with Tukey's multiple comparisons test. * $=p\leq 0.05$. **(D)** Neutrophils were treated with anti-human
823 Siglec-9 and Siglec-5/-14 antibodies (green) or media alone (purple) as in **C**. Cells were then
824 infected with sialylated (filled) or nonsialylated (empty) Gc at an MOI of 1. Survival of Gc as a
825 percent of the bacteria at time 0 min, as measured as in **Fig 3**. Statistical analyses by two-way
826 ANOVA with Holm-Šídák's multiple comparisons test. n=4 biological replicates (symbol
827 matched); * $=p \leq 0.05$, *** $p<0.0001$.

Figure 1

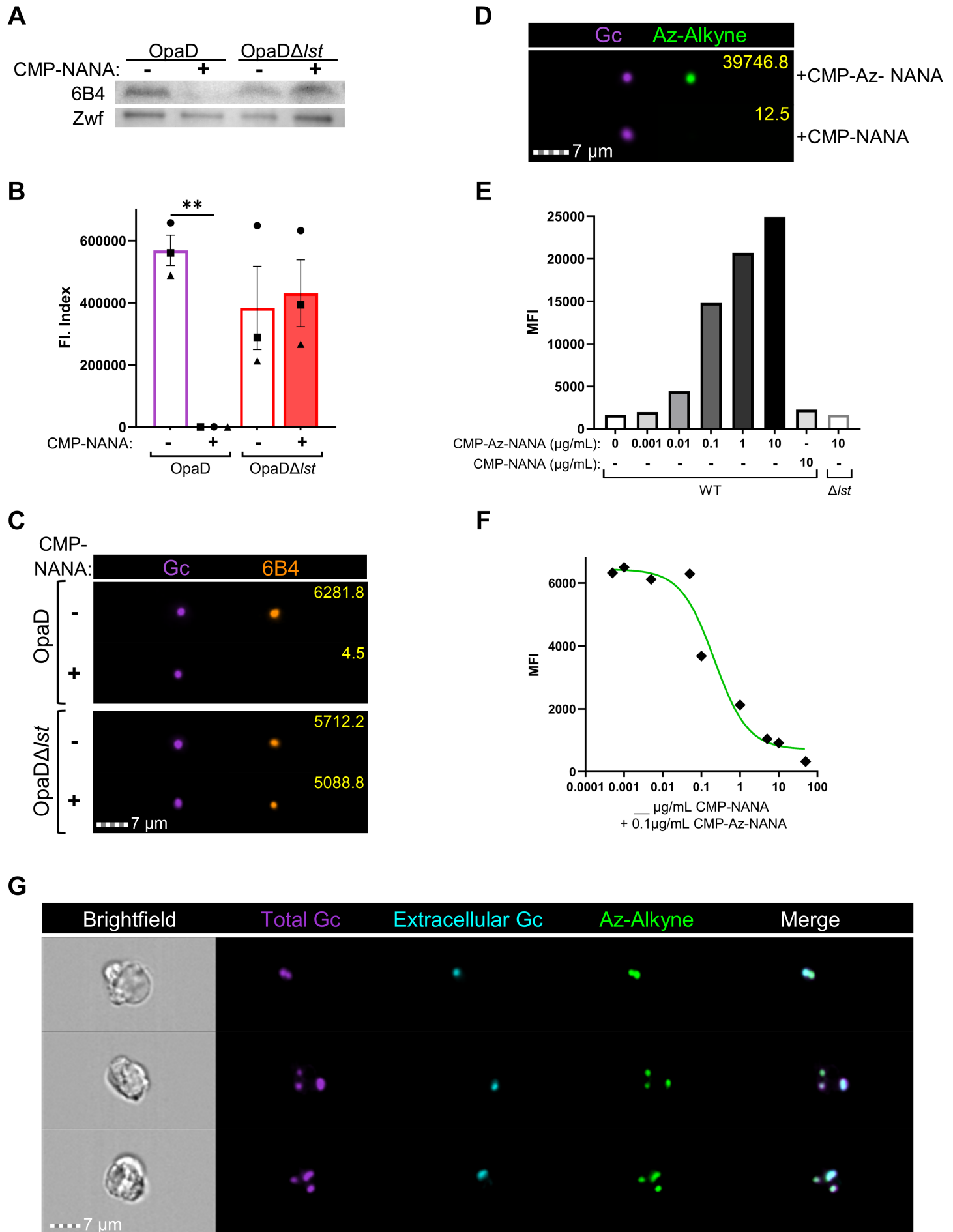


Figure 2

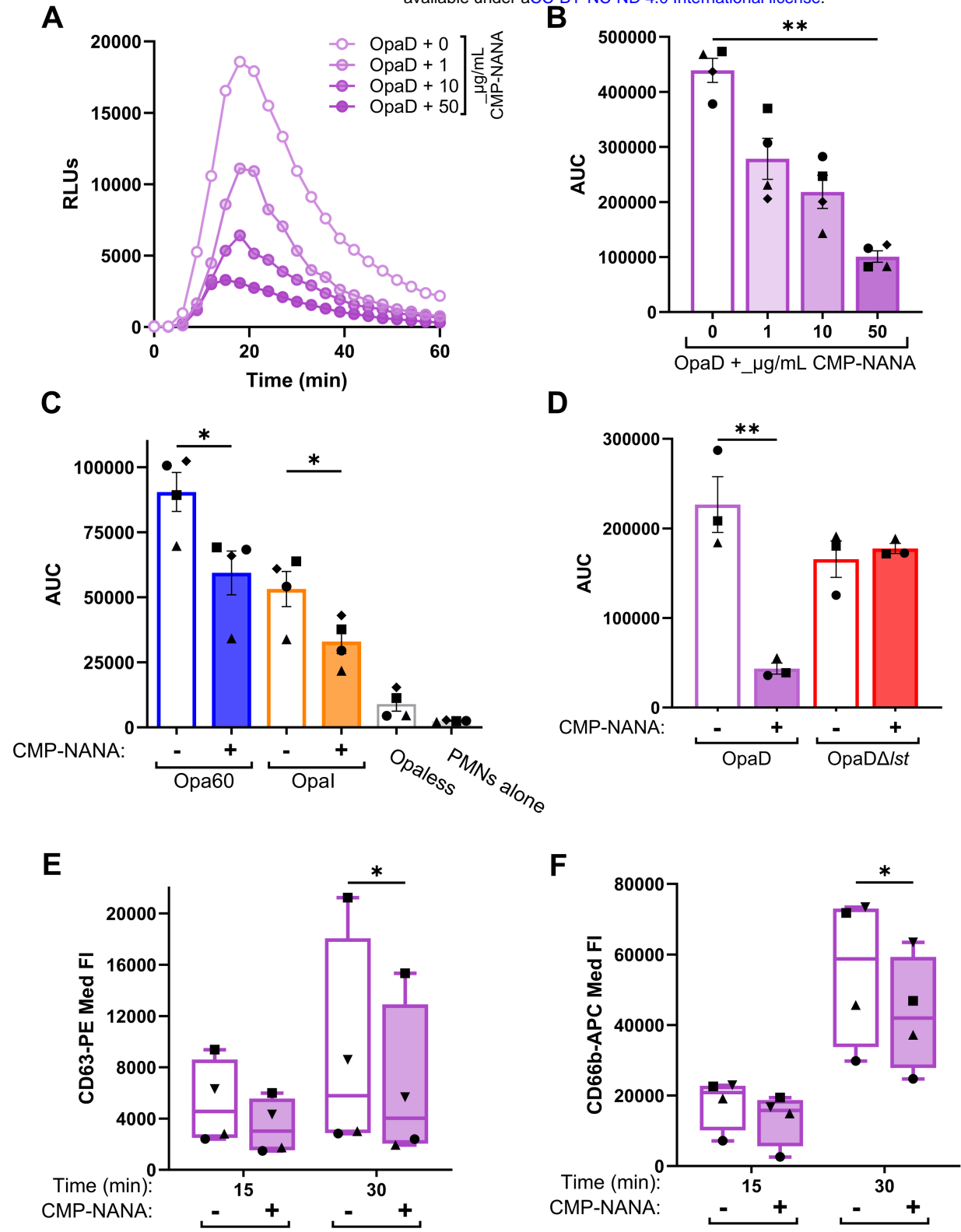
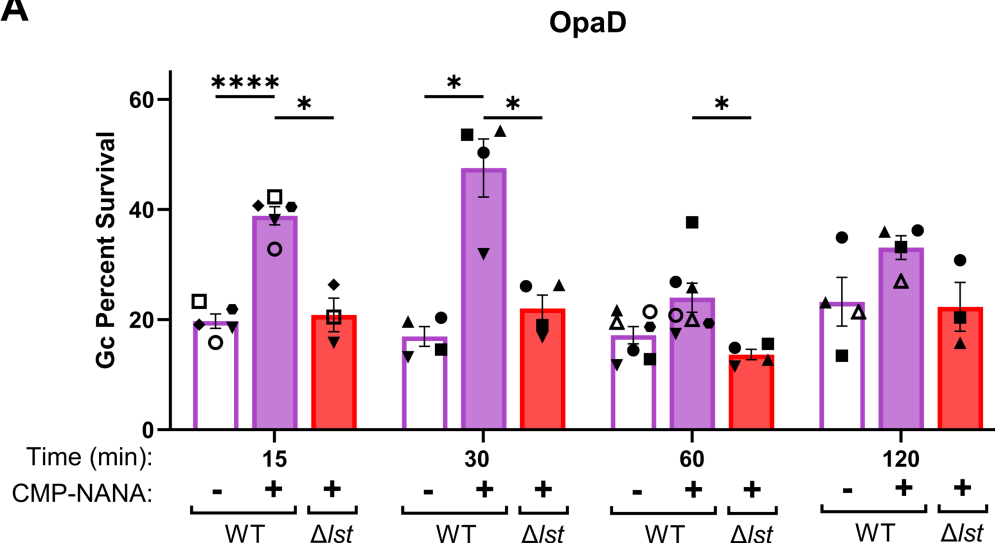


Figure 3

A



B

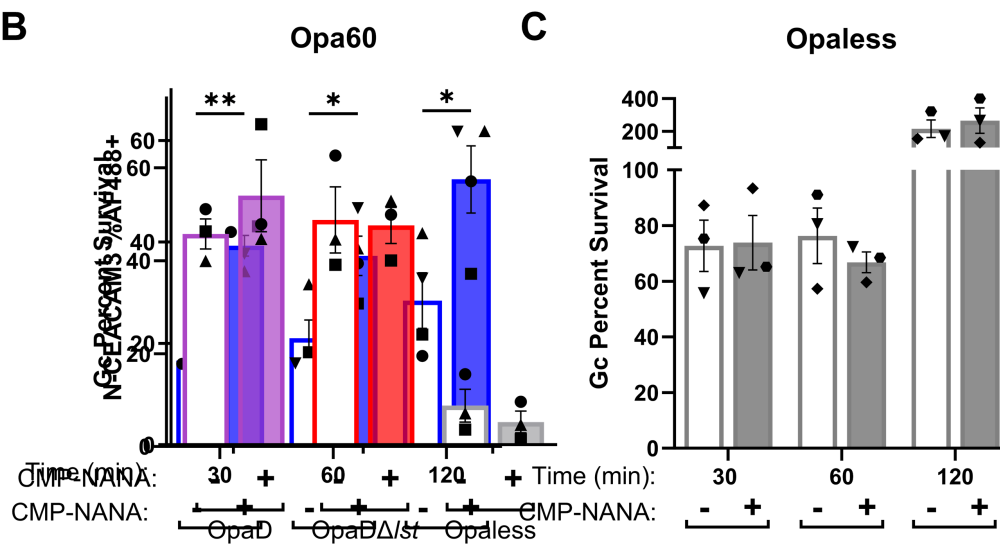
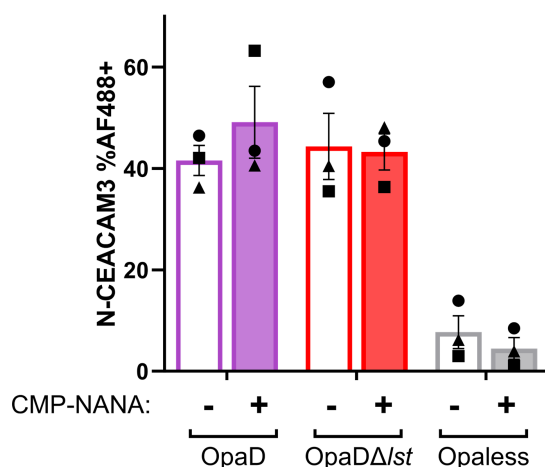
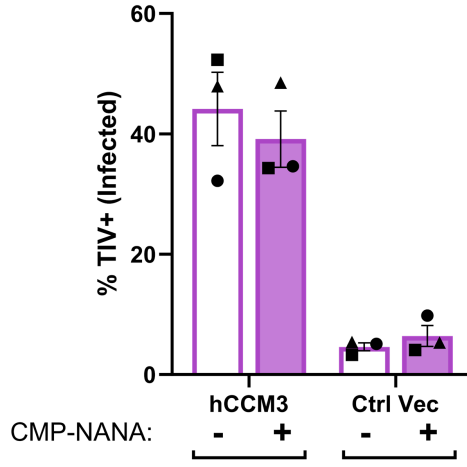


Figure 4

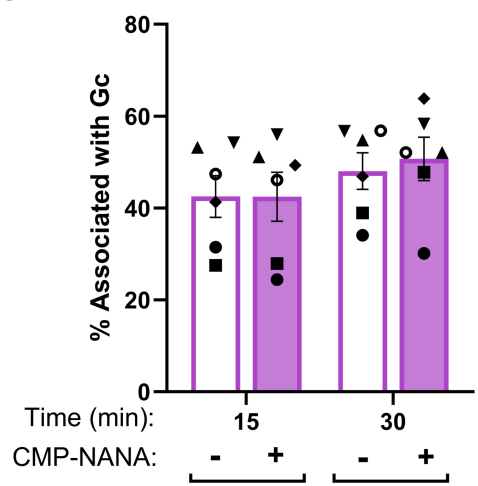
A



B



C



D

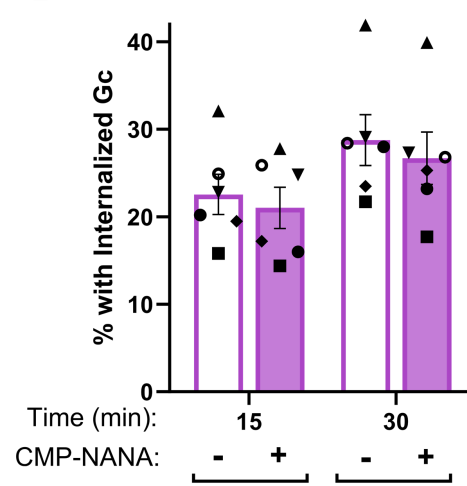


Figure 3

